Lasers in Manufacturing Conference 2015

One-Step Generation of Ultrahydrophobic Aluminum Surface Patterns by Nanosecond Lasers

R. Jagdheesh, J.J. García-Ballesteros and J.L. Ocaña*

UPM Laser Centre, Universidad Politécnica de Madrid
Ctra. de Valencia, km, 7.3, 28031, Madrid, SPAIN

Abstract

In recent years, metal surfaces that could mimic the water repellence properties of some natural surfaces have been the area of an intense research due to their potential applications such as self-cleaning, anti-contaminating and anti-sticking applications. Ultra short laser machining/structuring is a promising technique to obtain the dual scale roughness on the metal surface, which promotes the complex interfaces between solid-liquid-air, thus improves the wetting property of the surface. An attempt was made to study the improvement of wetting properties of aluminum by nanosecond laser source in one step process. Flat aluminum sheets of thickness 100 µm were laser machined with ultraviolet laser pulses of 30 ns with different laser parameters to optimize the process parameters. The samples produced at the optimum conditions with respect to contact angle measurement were subjected to microstructure and chemical analysis. The wetting properties were evaluated by static contact angle measurements on the laser patterned surface. The laser patterned microstructures exhibited ultrahydrophobic surface with a maximum contact angle of 180° for the droplet volumes of 8µL.

Ke*ywords Surface: Microstructuring, Ultrahydrophobic, Nanosecond Lasers.*

* Corresponding author. Tel.: +34 913363099,; fax: +34 913365535.
E-mail address: jlocana@etsii.upm.es.

1. *Introduction*

Wetting phenomena are significant in nature and technological industries. Superhydrophobic materials with micro or nano patterns on the metal surfaces find potential applications in home appliances, microelectronics, lab on chips, sensors etc. Various techniques based masking, laser direct writing process, and electrochemical techniques have been effectively implemented for micropattern the metallic surfaces (Jagdheesh, 2014; Pan, et al., 2009; Wang, et al., 2008). Micropattern with nano scale protrusions on the metal surface can alter the wetting properties of the metals from hydrophilic to superhydrophobic (Jagdheesh, et al., 2011). In common, two methods are widely accepted to generate the micro patterns, such as Top-down (Jagdheesh, 2014) and Bottom- up (Sanjay S. Latthe, et al., 2015) approaches. Bottom-up approaches has resulted in rectilinear features where as Top-down method has curvilinear features (Extrand, et al., 2014). Both these approaches are realized by several steps before the superhydrophobic property is achieved on the metal surface. The primary step is to create a periodic surface structure followed by surface activation by low energy materials (Jagdheesh, et al., 2011), this process is often termed as multiple step process. In one step process, the superhydrophobic surface is reached by creating periodic surface structure in single step process, eg. laser direct writing or laser ablation. Aluminum and its alloys are widely applied as structural engineering material due to its promising physical properties. The wetting property of aluminum alloy has been improved by anodization technique in single step. However, the duration of the process is about 120-150 minutes (Liu, et al., 2015). Chemical technique is also been employed for the transformation of the wetting property of commercially pure aluminum. J.Long et al. studied the improvement of wetting properties on aluminum by pico second induced micropattern with respect to time (Long, et al., 2015).

Micro and nano structured metal or ceramic surfaces; primarily hydrophilic has been transformed to hydrophobic or superhydrophobic with respect to time (Jagdheesh, 2014; Kietzig, et al., 2011). Several mechanisms have been suggested in literature for the transformation wetting property with respect to time, like partial deoxidation of CuO (Chang, et al., 2010) and decomposition of CO_2 into carbon (Anne-Marie Kietzig, et al., 2009). The change in the wetting property on the surface has been characterized by the static contact angle measurement (SCA). The SCA on the surface is estimated by the forces between liquid, solid and gas phases at the point of contact line. These forces are governed by roughness and surface tension of the material surface (Cassie, et al., 1944; Liu, et al., 2011). In spite of the available information on the various wetting transformation techniques in literature, the availability of nanosecond (ns) laser patterned ultrahydrophobic metal surface is very limited.

Although, laser pulses in nanosecond regime can produce defects in micromachining like, relatively large heat-affected zones, dross and recast, these laser sources are widely preferred in industry due to its well proven industrial robustness, large pulse energies and high pulse repetition rates, which provides accelerated machining process. The nanosecond laser processed structure/pattern of metals at ultra violet (UV) wavelength is one of the less explored aspect with respect to improvement of wetting properties. In this study, nanosecond laser pulses were applied on flat substrates of aluminum (Al) to fabricate micro pillars. Two different geometries such as micro channels and micro pillars have been studied with respect to the SCA. The resulted micropatterns were analyzed by scanning electron microscope (SEM) and confocal laser scanning microscope (CLSM) to evaluate the geometrical parameters of the structures.

2. Experiment

Flat aluminium, sheets of thickness less than 100 µm were micromachined by ultraviolet laser pulses. A Spectra-Physics laser source with nanosecond (ns) laser pulses, which has central wavelength of 1064 nm, was used. The fundamental frequency is 1064 nm was frequency-tripled (wavelength of 355 nm) by process of nonlinear optical conversion. The laser source has average maximum power of 20W at 100 kHz. The laser beam was guided over the samples surface by an optical system that included six mirrors, a beam expander, a digital scanner and a lens with 250 mm focal length. The experiments were performed at fixed pulse duration of about 30 ns. The laser beam has Gaussian power density profile and the machining was performed in atmospheric conditions with an apparent spot size of 15 µm. Two sets of samples were produced at a power 500 mW, with the geometry of micro-channels and micropillars. The microchannels and micropillars are separated by distance in a range of 10-25 µm. The distance is hereafter termed as pitch "P" for future reference in the text. The detailed laser processing conditions are listed in Table 1.

The laser machined surface patterns were analyzed with scanning electron microscope (SEM) attached with Energy dispersive X-ray spectroscope (HITACHI, Model S-3000N) and confocal laser scanning microscope (CLSM) to evaluate the geometry of the microholes. The hydrophobicity/water repellence of the samples was studied by measuring the static contact angle using the sessile drop technique, with a video-based optical contact angle measuring device (OCA 15 plus from Data Physics Instruments). 8 µL droplet of distilled deionized water was dispensed on the laser-machined surface structures under atmospheric conditions, and the static contact angle was calculated by analyzing droplet images recorded just after the drop deposition.

Table 1. : Laser Processing parameters

Pitch, P (*µm)*	10, 15, 20, 25
Laser Power (mW)	300
Repetition rate (kHz)	100
Scan Speed (mm/s)	40

3. Results and Discussion

Micro channels and micro pillars have been fabricated with process parameters shown in Table 1. Figure 1 represents the CLSM 3D image of the micro channels fabricated with four P : 10, 15, 20 and 25 µm. The width of the channel measurements is about of 3, 5, 7 and 8 µm corresponding to the P value, 10, 15, 20 and 25 µm. All the micro channels recorded a depth in the range of 1.75-2.75 µm. The melt and recast formation is unavoidable in nano second laser processing. The depth of the micro channels should be constant irrespective of the pitch distance. The depth difference may be related to the fact that, molten materials coming from the subsequent channels would partially fill the previously fabricated channels. Moreover, the difference in the depth could also be related to the height of the piled recast layer or micro-wall like structure above the substrate surface. The height and width of the micro wall is influenced by the overlap of the recast layer formed on the adjacent micro channel edges. Further, The channels fabricated by P : 10 and 15 µm resulted into near broken state. The height of the micro-wall is influenced by melt ejection and the repeated melting of the recast by the low power density tail end of the Gaussian beam profile.

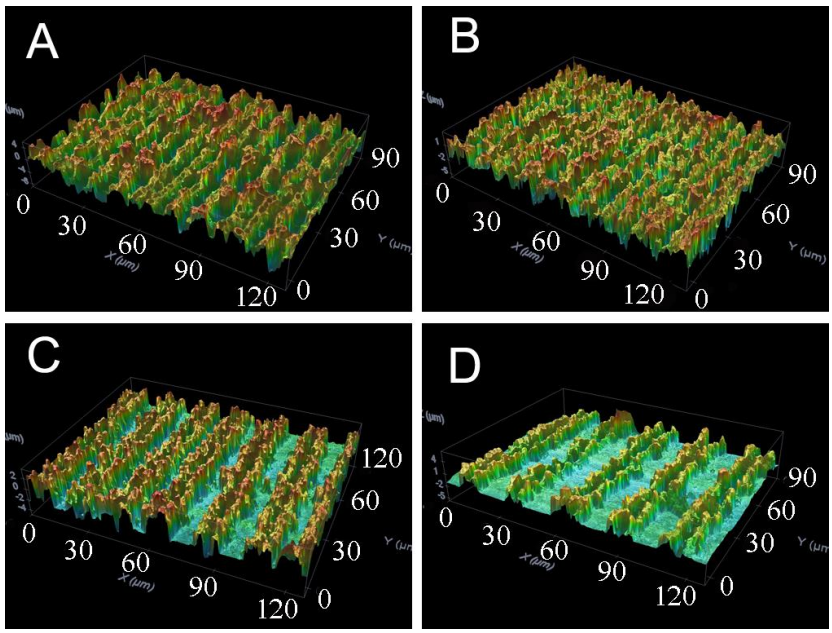

Fig. 1. CLSM 3D image for the microchannels fabricated with, P: 300 mW, scan speed: 40mm/s and repetition rate : 100 kHz for four different P; A):10 µm; B):15 µm; C):20 µm; D):25 µm.

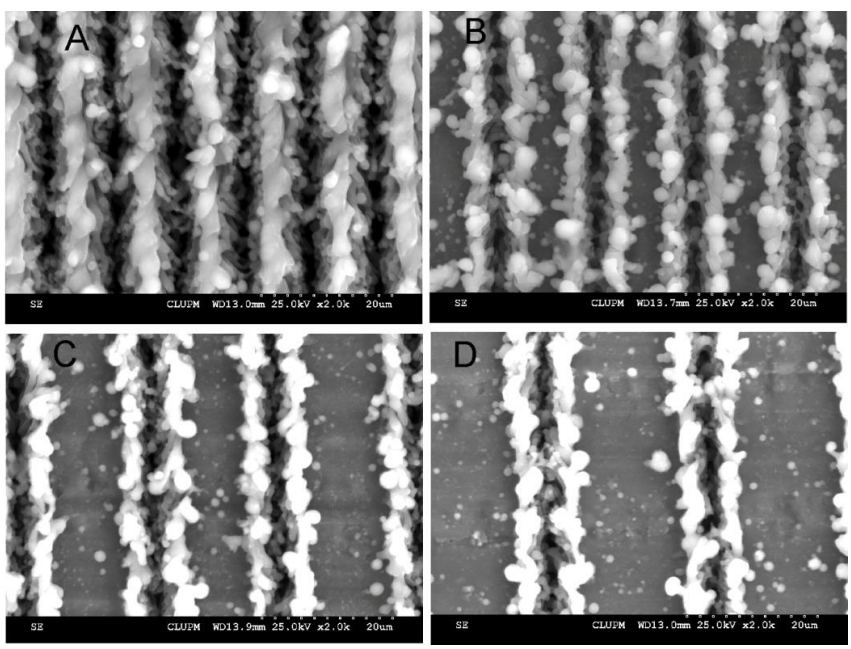

Fig.2. SEM image for the microchannels fabricated with, Power : 300 mW, scan speed: 40mm/s and repetition rate : 100 kHz for four different P; A):10 µm; B):15 µm; C):20 µm; D):25 µm.

From the confocal image, it is apparent that, the surface has high density of debris on the surface, which is resulted due to splashing of the molten material and redeposition from the vaporized material. This sample exhibited relatively high hydrophilicity immediately after machining and the degree of hydrophobicity has been improved with respect to time. Figure no.2 represents the SEM images of micro channels fabricated with the power of 300 mW. The formation of the recast layer is along the direction of laser machining. For the sample machined with P: 10 µm, the small horizontal shift has produced very narrow micro channel, with the effective average channel width of 1.75 µm. The narrow width and reduced height can be attributed repeated melting of the recast layer by the tail end of the Gaussian beam profile. The sample machined with P of 15, 20 and 25 µm has untreated metal surface between the channels and the micro channels has higher depth (2 - 2.75 µm).The improvement in the depth of the microchannels is attributed to the increase in the height of the micro walls.

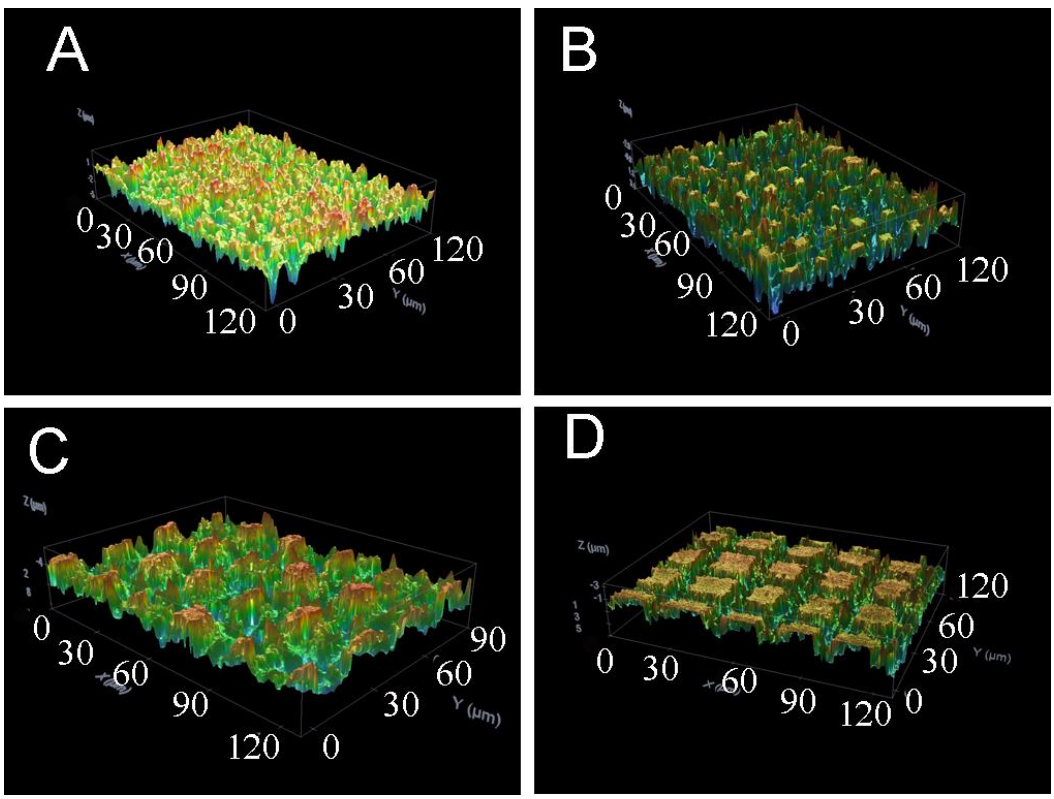

Fig.3. CLSM 3D 3D image for the micro-pillars fabricated with, P: 300mW, scan speed: 40mm/s and repetition rate : 100kHz for four different P: A):10 µm; B):15 µm; C):20 µm; D):25 µm.

Unlike the sample treated with P: 10 µm, the presence of spherical shaped particle on the top of the recast layer has been observed. The spherical shaped particle is a result of resolidification of metal vapour caused due to the ablation mechanism. Further, the aluminium surfaces have the debris spread over the unprocessed aluminium surface. The recast materials from the adjacent microchannels form an additional channel on the top surface with height in submicron range. This submicron channels is advantageous with respect to improvement of hydrophobicity of the metal surfaces.

Figure 4 shows the confocal 3D image of the micro pillars fabricated with four P: 10, 15, 20 and 25 µm with 300 mW laser power. The micro pillars fabricated with P: 10 and 15 µm resulted into scattered peak instead of peaks at regular intervals. It is observed that, heavy deposition recast material on the top surface of the micro pillars. Whereas, the micro pillars fabricated with P of 20 and 25 µm have deposition over the circumference of the micro pillars. The SEM (fig.4) images recorded for the micro pillars generated with 300 mW laser power, indicates the melt formation during the laser ablation. It is clear that, the molten material solidifies along the direction laser movement. For all the four P, the channels are opened in one direction and closed on the other direction. This is caused by the ejection of the melt formed during the laser processing. In addition to the heavy piling up of recast material on the top edges of micro pillars, spherical shaped resolidified metal vapour structures are also found. This may be the self-cooled metal vapour from the plasma generated by laser ablation.

The piling of the recast forms a µ-cell or closed packet like structure on the top of the micro pillars as shown in fig.5. The µ-cell structure is separated by 10-15 µm channels. Therefore, the laser patterned aluminium surface has two different patterns such as micro pillars and µ-cell. Thus, reducing the fraction of solid area in contact with the water droplets. This is an advantage as for as water repellence is concerned. The closed micro channels act as micro packets and it can hold small volume of air trapped inside the pockets. This would prevent the water to flush out the air inside the narrow micro channels.

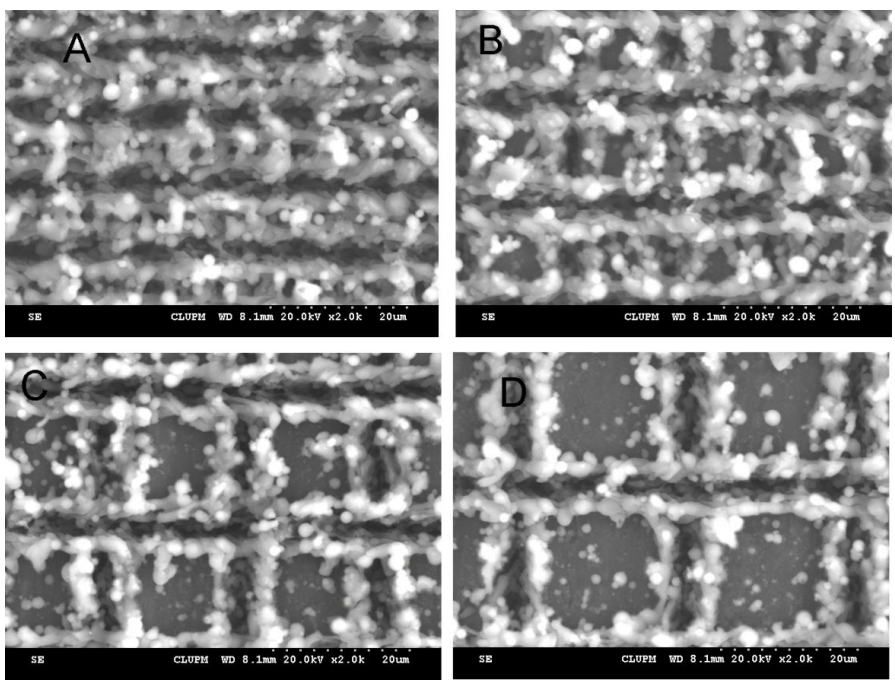

Fig.4. SEM image of micro pillars fabricated with, Power: 300 mW, scan speed: 40 mm/s and repetition rate : 100kHz for four different P; A):10 µm; B):15 µm; C):20 µm; D):25 µm.

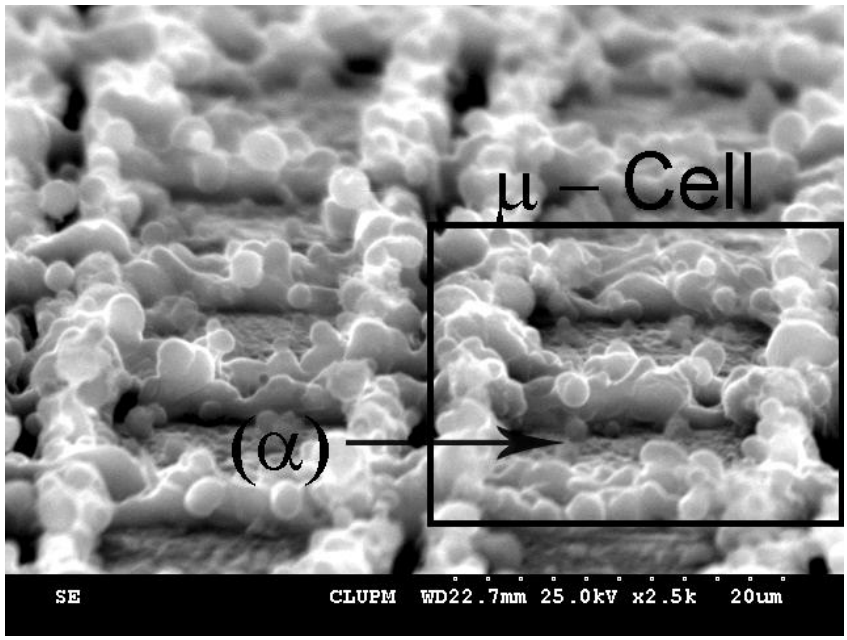

Fig.5. SEM image of μ-cell formation on top of the micro pillars (P:25 μm)

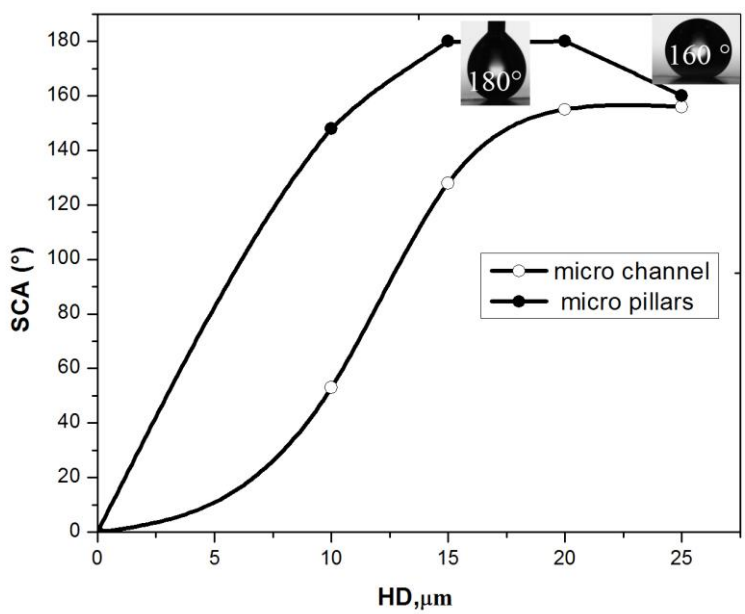

***Fig.6**.Static contact angle for the micro channels and micro pillars as a function hatch distance.*

The effect of micro patterns on the wetting properties of the Al samples was evaluated by static sessile drop contact angle measurements, using a droplet size of 8 µL. The plain Al surface recorded a SCA value of 85 ±3°. The entire laser patterned surface was highly hydrophilic within minutes of processing. The SCA measurements were unable to be computed due to very low CA values (less than 30°). However, the measurements performed after 24 hours exhibited the hydrophobic character. The SCA measurements shows increase in SCA values with respect to P and starts declination beyond P: 20 µm for micro pillar structures. The SCA measurements on micro channel patterns shows the similar trend like micro pillars and it saturates as the P is increased beyond 20 µm. For the cases, where the water droplets are unable to dispense or land on the surface from the microsyringe, the normal sessile droplet technique is not applicable. The SCA of these kind of surface is considered to be 180° (Zhang, et al., 2007) or ultrahydrophobic surface. The low values of SCA for the sample processed with P: 15 µm may be due to the non-formation of µ-cell structure. Samples with micro pillar geometry exhibited ultra ultrahydrophobicity for the samples processed with P: 15 and 20 µm. The sample processed P : 25 µm recorded a SCA of 160°. When the droplet is dispensed on the laser patterned surface, the water droplet has contact only with the top edge of the µ-walls due to the small volume of air trapped in the µ-cell structures. The air bubbles act as cushion for the water droplet. Thus avoids the contact with the bottom surface of the µ-cell structures.

The ultrahydrophobicity of the micro patterns may be attributed to the formation of µ- cell structure on the top of the micro pillars. The micro pillar geometry recorded a decline in SCA values, as the P is increased from 20 µm. The reduction may be due to the increase in spacing between the µ- cell structures. When a water droplet is dispensed on the surface it wets the hydrophilic surface (which is marked as (α) on the top of the micro pillar, fig. No.5) and dewets the ultrahydrophobic µ walls. Therefore, when the P is increased, the water is exposed to the larger hydrophilic surface (α), and tends to land on the surface resulting a SCA of 160°. In general, the laser processed surface structures are found to be composed of curvilinear features. The formation of µ-cell structure suppresses the curvilinear features and it has become more rectilinear. The magnitude capillary forces action around µ- cell features must be directed upward and it is greater than the downward forces resulting from gravity, inertia and Laplace curvature, giving a cassie state of wetting (Cassie, et al., 1944).

4. Conclusions.

Thin sheets of aluminium are micromachined with ultraviolet laser pulses of 30 ns, to create ultrahydrophobic surface in one-step direct writing technique. The melting effect is well pronounced for the laser pattered structures. The results show that, the micro pillars and the formation of the µ-cell by laser processing plays a significant role in improving the degree of hydrophobicity. The typical laser processed curvilinear structure has been replaced by rectilinear µ-cell structures. Laser processed micropillars exhibited ultrahydrophobic surface with SCA measurement of 180°. The SCA values are very consistent for repeated measurements at the same spot.

Acknowledgments

The authors are thankful to BSH Electrodomésticos España S.A., for their support in executing this work.

References

Anne-Marie Kietzig, Savvas G. Hatzikiriakos, and Peter Englezos, 2009, Patterned Superhydrophobic Metallic Surfaces, Langmuir, 25, p. 4821-4827

Cassie, A. B. D., and S. Baxter, 1944, Wettability of porous surfaces, Transactions of the Faraday Society, 40, p. 546-551

Chang, Feng-Ming, Shao-Liang Cheng, Siang-Jie Hong, Yu-Jane Sheng, and Heng-Kwong Tsao, 2010, Superhydrophilicity to superhydrophobicity transition of CuO nanowire films, Applied Physics Letters, 96, p. 114101

Extrand, C. W., and Sung In Moon, 2014, Repellency of the Lotus Leaf: Contact Angles, Drop Retention, and Sliding Angles, Langmuir, 30, p. 8791-8797

Jagdheesh, R , B. Pathiraj, E. Karatay, G.R.B.E Romer, and A.J Huis in't Veld, 2011, Laser-Induced Nanoscale Superhydrophobic Structures on Metal Surfaces, Langmuir, 27, p. 8464-8469

Jagdheesh, R., 2014, Fabrication of a Superhydrophobic Al2O3 Surface Using Picosecond Laser Pulses, Langmuir, 30, p. 12067-12073

Kietzig, Anne-Marie, Mehr Negar Mirvakili, Saeid Kamal, Peter Englezos, and Savvas G. Hatzikiriakos, 2011, Laser-Patterned Super-Hydrophobic Pure Metallic Substrates: Cassie to WenzelWetting Transitions, Journal of Adhesion Science and Technology, 25, p. 23

Liu, K, and L Jiang, 2011, Metallic surfaces with special wettability Nanoscale, 3, p. 825-838

Liu, Yan, Jindan Liu, Shuyi Li, Yaming Wang, Zhiwu Han, and Luquan Ren, 2015, One-step method for fabrication of biomimetic superhydrophobic surface on aluminum alloy, Colloids and Surfaces A: Physicochemical and Engineering Aspects, 466, p. 125-131

Long, Jiangyou, Minlin Zhong, Hongjun Zhang, and Peixun Fan, 2015, Superhydrophilicity to superhydrophobicity transition of picosecond laser microstructured aluminum in ambient air, Journal of Colloid and Interface Science, 441, p. 1-9

Pan, Qinmin, and Yuexiang Cheng, 2009, Superhydrophobic surfaces based on dandelion-like ZnO microspheres, Applied Surface Science, 255, p. 3904-3907

Sanjay S. Latthe, Sudhagar P, Ravidhas C, A. Christy Jennifer, D.Kirubakaran David, Venkatesh R, Anitha Devadoss, C Terashima, K. Nakataac, and Akira Fujishimaac, 2015, Self-cleaning and superhydrophobic CuO coating by jet-nebulizer spray pyrolysis technique, CrystEngComm, 17, p. 5

Wang, Qi, Bingwu Zhang, Mengnan Qu, Junyan Zhang, and Deyan He, 2008, Fabrication of superhydrophobic surfaces on engineering material surfaces with stearic acid, Applied Surface Science, 254, p. 2009-2012

Zhang, Jihua, Xuefeng Gao, and Lei Jiang, 2007, Application of Superhydrophobic Edge Effects in Solving the Liquid Outflow Phenomena, Langmuir, 23, p. 3230-3235